Circulation
Volume 92, Issue 10, 15 November 1995; Pages 3122-3131
https://doi.org/10.1161/01.CIR.92.10.3122

ARTICLE

Effects of Anterior Communicating Artery Diameter on Cerebral Hemodynamics in Internal Carotid Artery Disease

A Model Study

Francis Cassot, Valérie Vergeur, Philippe Bossuet, Berend Hillen, Mokhtar Zagzoule, and Jean-Pierre Marc-Vergnes

ABSTRACT: *Background* Collateral circulatory pathways are considered the primary determinant of cerebral hemodynamics in patients with obstructive lesions of the internal carotid arteries (ICaAs). However, the hemodynamic effects of the diameter of the anterior communicating artery (ACoA) have never been assessed quantitatively in humans. *Methods and Results* Two different mathematical models were used to simulate changes affecting blood pressures and flows in cerebral arteries as a function of ACoA diameter and ICaA stenoses or occlusions. Small changes in ACoA diameter were found to have marked hemodynamic effects when they occurred within the range of 0.4 to 1.6 mm, a situation observed in 80% of the cases. Outside this range, changes in ACoA diameter had no effect. Simulated pressure drops through a stenotic ICaA were consistent with those observed. They were found to depend on the degrees of the stenoses in both ICaAs and on ACoA diameter

according to a simple equation. Pressure reserve in the middle and anterior cerebral arteries decreased to below the lower limit of autoregulation, despite a normal mean arterial blood pressure, when the arteries were distal to a unique 70% ICaA stenosis associated with a small-diameter ACoA or to a 50% ICaA stenosis associated with a contralateral ICaA occlusion and a large-diameter ACoA. Above these thresholds, the circle of Willis allowed for an almost complete global cerebral blood flow compensation that involved all the afferent and communicating vessels. *Conclusions* ACoA diameter strongly modulates the effects of ICaA lesions on cerebral hemodynamics. Some proposals for endarterectomy indications can be derived from our study.

Key Words: stenosis ■ blood pressure ■ carotid arteries ■ cerebrovascular disorders ■ computers

---

Occlusions and severe stenoses of the ICaAs have been shown to induce net changes in cerebral hemodynamics. These changes include an increase in the CBV and the ratio of CBV to CBF (CBV/CBF),[1 2 3 4 5 6 7] as well as a decrease in the CBF reactivity to vasodilatory stimuli such as CO_2[8 9 10 11] or acetazolamide.[12 13 14] A good correlation has been found between these parameters.[15] Furthermore, in animals, CBV changes have been shown to be closely related to changes in MABP.[16] Thus, the hemodynamic abnormalities distal to a severe ICaA lesion are considered to be due to the reduction in CPP induced by the lesion and to the autoregulatory vasodilation of the cerebral vascular network. However, on an individual level, “the degree of carotid

stenosis correlates poorly with the hemodynamic status of the ipsilateral cerebral circulation. The primary determinant of cerebral perfusion pressure and blood flow under these circumstances is the adequacy of collateral circulatory pathways," as pointed out by Powers in a recent review article.[17] A similar statement was made by Schroeder in another review article.[18] Only indirect evidence[1 2 9 11] supports this conclusion. Any experimental approach to the relation between the functional status of collateral circulatory pathways and CPP is limited by two factors. First, the CBV/CBF ratio is a rather gross estimate of the local pressure gradient; second, the circle of Willis, which is the main anastomotic pathway in the cerebral circulation, is located deep in the base of the skull, and its morphometry and functional status have never been assessed directly and quantitatively in humans.

Modeling the cerebral circulation is an alternative approach to study the relation between the functional status of collateral circulatory pathways and CPP. The flow of blood in the cerebral network, even though it is strongly modulated by the motor function of the cerebral arteries, remains basically subject to the rules of fluid mechanics. Thus, it has been possible to develop mathematical models that simulate the cerebral circulation and allow calculation of the values of all the parameters of interest under various conditions in animals[19 20 21] and in humans.[22 23 24] Therefore, as a first attempt, we adapted two models described previously[23 24] to study the effect of the diameter of the ACoA on cerebral hemodynamics in the presence of stenotic and/or occluded internal carotid arteries. To the best of our knowledge, this effect has never been studied specifically, whereas the morphometric variations of this artery are well established. In the present study, emphasis was placed on the

changes in blood pressure in the circle of Willis and its afferent and efferent branches.

METHODS

Our first model (Fig 1) was derived from that proposed by Zagzoule and Marc-Vergnes[23] and includes the two ICaAs, the two vertebral arteries, the BA, the first segments (7 cm) of the two ACeAs, MCeAs, and PCeAs, the ACoA, and the two PCoAs.

Blood flow through this distensible network was simulated by use of unsteady fluid mechanics equations: conservation of mass and of momentum and a tube law relating internal blood pressure to arterial cross-sectional area (see “Appendix”). The viscous term in the momentum equation (see “Appendix”) was computed from a time-dependent expression.[25] Blood was considered to be a homogeneous incompressible newtonian fluid and the arterial wall to be purely elastic. The unsteady set of equations governing blood and arterial wall motion were solved numerically by the two-step Lax-Wendroff scheme.[23] Given the pressure at the entry of the four afferent vessels and the peripheral resistances at the output of the six efferent vessels, the model computes pressure, flow, and wall shear-stress values at any point of the network.

This nonlinear unsteady model was applied to the morphometric data (Table 1) already used by Hillen et al[26] and by Zagzoule and Marc-Vergnes.[23] The calculations were initiated at the diastolic pressure, the pressure signal used by Hillen et al[26] being taken as proximal boundary conditions. Stenoses of various degrees expressed as percent narrowing in the luminal diameter were added to one or both ICaAs over a 5-cm length. The local hydrodynamic effects induced by an ICaA stenosis were predicted with a

semiempirical law, established in vitro by Young and Tsai[27] and validated in vivo by Young et al,[28] that relates the pressure drop to the unsteady flow velocity. Changes in ACoA diameter were introduced within the range of 0 to 3.0 mm. The diameter of both PCoAs was kept constant at 1.0 mm.

Second, we compare the results obtained by this nonlinear unsteady model with those provided by a simpler linear network model, which has been shown previously to behave in a way similar to the reference model.[24] The mathematical formulation of this linear model was established by writing the flow balance at each node of the network, ie, at each junction of the circle of Willis. This leads to a set of nine linear algebraic equations for the nine unknown nodal pressures (see “Appendix”), which can be solved either numerically by standard techniques or analytically with the software package for symbolic calculus MAPLE V, provided that the input pressures at the entry of the carotid and vertebral segments and the peripheral resistances are known.

RESULTS

Blood Pressure

The first parameter to be computed was the mean pressure drop through an ICaA stenosis because it is the only pressure value in the human brain circulation that is measured currently and directly during endarterectomy. In Fig 2, its predicted values are plotted against the degree of ICaA stenosis for different ACoA diameters. An S-shaped curve is obtained for each value of ACoA diameter. As long as the degree of stenosis remains <30%, the mean pressure drop does not change significantly from the normal value of 2.5 mm Hg for any ACoA diameter. As the degree of stenosis increases from

30% to 90%, the pressure drop increases with the degree of stenosis, but the slope of the curve is strongly affected by the ACoA diameter: for instance, with a 70% ICaA stenosis, the pressure drop goes from 10 to 36 mm Hg when the ACoA diameter decreases from 2.0 to 0 mm. ICaA stenoses >90% have no further effect on the pressure drop.

Fig 3 illustrates the effects of changes in ACoA diameter on the transstenotic pressure drop. The effects differ according to whether the ACoA diameter varies outside or within the range of 0.4 to 1.6 mm. Outside this range, ACoA behaves either as a fully efficient vessel if its diameter is ≥1.6 mm or as an entirely inefficient one if its diameter is ≤0.4 mm. Within this range, the MABP distal to an ICaA stenosis >40% is strongly modulated by the ACoA diameter. For instance, an ICaA occlusion induces a pressure drop that is 4-fold or 20-fold its normal value when the ACoA diameter is 1.6 or 0.4 mm, respectively.

In fact, there is a coupling effect involving both parameters, ie, the degree of ICaA stenosis and the ACoA diameter. An accurate representation of the mechanism of this interaction is schematized in Fig 4. The vascular network behaves like a very simple electrical circuit, the input of which (the “voltage”) is the pressure drop of the network with a fully efficient ACoA for the given stenosis (this value can be read on the lower curve in Fig 2), while the output gives the real pressure drop. This circuit is made of two parallel lines whose outputs are summed. On one line, the input value is identically transmitted, while on the other, it is multiplied by two amplifiers in a cascade. The gain of the first amplifier (Gs) varies with the degree of stenosis, increasing from 0 to 3.42, following an S-shaped curve; the gain of the second amplifier decreases with the ACoA diameter from 1 to 0, being equal to unity for any ACoA diameter <0.4 mm and to

zero for any ACoA diameter >1.6 mm. The same mechanism holds for bilateral stenoses. The range of Gs remains the same (between 0 and 3.42) as in the unilateral case. However, the response Gs of the “stenotic” amplifier in this case, as well as the input “signal,” depends on degrees of both stenoses.

Indeed, this qualitative behavior of the transstenotic pressure drop, as a function of the stenotic configuration and of the ACoA diameter, can be deduced directly from the analytical solution of the linear model. From this simplified model, the transstenotic pressure drop can be expressed algebraically in terms of the conductances of the ACoA and of the stenotic ICaA. For instance, for an unilateral stenosis, it can be shown that this pressure drop has the form

\batchmode \documentclass[fleqn,10pt,legalpaper]{article} \usepackage{amssymb} \usepackage{amsfonts} \usepackage{amsmath} \pagestyle{empty} \begin{document} \[{\Delta}P\ {=}\ {\Delta}P_{{\infty}}\frac{{\alpha}_{0}\ {+}\ G_{CoA}}{{\beta}_{0}\ {+}\ G_{CoA}}\] \end{document}

where ΔP denotes the transstenotic pressure drop, ΔP_{∞} is its corresponding value for a large ACoA, G_{CoA} is the ACoA conductance, α_0 is a constant for a given network, and β_0 depends on the conductance (G_{st}) of the stenotic ICaA, expressed as

\batchmode \documentclass[fleqn,10pt,legalpaper]{article} \usepackage{amssymb} \usepackage{amsfonts} \usepackage{amsmath} \pagestyle{empty} \begin{document} \[{\beta}_{0}\ {=}\ \frac{b_{0}\ {+}\ b_{2}G_{st}}{b_{1}\ {+}\ b_{3}G_{st}}\] \end{document}

where b_0, b_1, b_2, and b_3 are constants.

If this pressure drop were plotted versus the ACoA diameter or the degree of stenosis, exactly the same type of S-shaped curves that were found with the numerical model would be obtained.

The second pressure parameter computed was the pressure at the entry of the cerebral arteries. It was expressed in terms of “mean pressure reserve,” defined here as the difference between the absolute pressure at the given artery and the capillary pressure taken to be equal to 35 mm Hg. The lower limit of autoregulation in the territory supplied by the artery is reached when this pressure reserve equals 23 mm Hg (see “Discussion”). Fig 5 shows that the relation between the mean pressure reserve at the entry of the MCeAs and the severity of the ICaA stenotic configuration is not linear and can be described by a double S-shaped curve on both the ipsilateral and the contralateral sides with respect to the main ICaA lesion.

In the MCeA ipsilateral to the main ICaA lesion (Fig 5, left), the pressure remains nearly constant when the ICaA configuration ranges from that of a unilateral 80% stenosis to that of an occlusion with a contralateral 15% stenosis, and the level of the plateau depends on both the MABP and the ACoA caliber. For instance, as the MABP decreases from 100 to 80 mm Hg, the pressure reserve in the MCeA decreases from 54 mm Hg (point A, Fig 5 left) to 36 mm Hg (point B, Fig 5 left) for a unilateral stenosis and an ACoA diameter of 2 mm. However, whatever the MABP, the caliber of the ACoA has a crucial effect on the pressure reserve at the entry of the MCeA ipsilateral to the main ICaA lesion. When the ACoA is fully patent, the lower limit of autoregulation is reached in an MCeA territory only if an ipsilateral occlusion is associated with a contralateral stenosis of 55% (point C, Fig 5 left) or 70% (point C′, Fig 5 left) according to the MABP. When the ACoA is inefficient, this

lower limit is reached in the same territory as long as a unilateral ICaA stenosis reaches a value of 65% (point D, Fig 5 left) or 75% (point D′, Fig 5 left), according to the MABP.

At the entry of the MCeA contralateral to the main ICaA lesion (Fig 5, right), the pressure reserve remains constant for an ICaA configuration of a unilateral stenosis ranging from 50% to 100% (occlusion), and the level of the plateau depends mainly on the MABP. The lower limit of autoregulation is reached in this territory when the ICaA stenosis contralateral to an ICaA occlusion varies from 35% (point E, Fig 5, right) to 50% (point E′, Fig 5, right) at any MABP and ACoA diameter. Similar results were obtained for the ACeAs.

Fig 6 summarizes all the results by giving the lowest MABP value that allows autoregulation to occur in both ipsilateral and contralateral MCeA territories according to the degrees of stenosis in the ipsilateral and contralateral ICaAs and for four values of ACoA caliber. For instance, in a model with an ACoA caliber of 0.7 mm (second panels from bottom), an 80% ipsilateral ICaA stenosis, and a 40% contralateral ICaA stenosis, the lower limit of autoregulation is reached in the MCeA territory ipsilateral to the main stenosis when the MABP equals 90 mm Hg and in the MCeA territory contralateral to the main stenosis when the MABP equals 67 mm Hg. In the case of bilateral ICaA occlusion, the lower limit of autoregulation occurs at a MABP of 120 mm Hg. In a similar way, one can read on this figure the lowest MABP value enabling an efficient autoregulatory response at the MCeA level for any possible combination of unilateral or bilateral stenoses, depending on the ACoA diameter.

Cerebral Blood Flow

Since our model does not simulate the autoregulatory vasodilation that occurs in the resistive cerebral arteries when the arterial blood

pressure decreases, the values of CBF reported here are underestimated. They only give some insight into the compensatory capacity related to the anatomic features of the arterial network.

As expected, each reduction of vessel diameter induces a decrease of the tCBF through the entire network. In our model of normal circulation, with a MABP of 100 mm Hg, the tCBF equals 723 mL/min, including 247 mL/min through each ICaA and 229 through the BA (Table 2A). When a unilateral ICaA stenosis is added to the model, tCBF decreases slightly and equals 689 mL/min (−4.7%) for a unilateral ICaA occlusion (Table 2B). An additional reduction of the ACoA diameter to 0.5 mm (Table 2D) has an effect similar to that of an additional 50% contralateral ICaA stenosis with ACoA diameter kept at 1.6 mm (Table 3A), ie, a tCBF decrease to 602 mL/min (−17% compared with normal). When both ACoA diameter reduction and contralateral ICaA stenosis are added to the model, tCBF decreases to only 563 mL/min (−22%), showing that these effects are not cumulative (Table 3C).

The anastomotic phenomena that compensate for the flow deficit in a vessel involve all the afferent and communicating arteries of the circle of Willis but are strongly dependent on the ACoA diameter (Table 2).

In a model configuration of a unilateral ICaA lesion with a normal ACoA diameter, ie, ≥1.6 mm (Table 2B), the flow in the contralateral normal ICaA increases from 247 to 429 mL/min (+73.7%) as the degree of stenosis increases. At occlusion, 199 of these 429 mL/min, ie, 47.3% of the total flow of this vessel, goes through the ACoA to the occluded side. Consequently, the ACeA and MCeA of the nonoccluded side receive only 230 mL/min and an additional 2 mL/min through their ipsilateral PCoA from the BA. The flow in this artery increases only from 229 to 259 mL/min (+13.1%), 21 mL/min

of which flows to the occluded side through the corresponding PCoA. In this configuration, the occluded side receives 90.5% of its supply from the contralateral ICaA and 9.5% from the BA, a figure subject to changes strongly depending on the diameter of the PCoA, the effects of which were not studied here. In the same configuration of a unilateral ICaA lesion but with an ACoA diameter reduced to 0.8 mm (Table 2C), an occlusion causes the flow in the contralateral ICaA to increase to 339 mL/min (+37%). In this case, 97 mL/min, ie, 28.6% of the total flow in this vessel, flows to the occluded side through the ACoA. The flow in the BA increases to 298 mL/min (+30%), of which 70 mL/min flows to the occluded side through the corresponding PCoA. Thus, the blood supply to this side, which is only 68% of the normal value, comes from the contralateral ICaA (58%) and from the BA (42%). Below a threshold ACoA diameter of 0.75 mm, the carotid territory distal to an ICaA occlusion receives more supply from the BA than from the contralateral ICaA. For instance, when the ACoA diameter equals 0.5 mm, ≈80% of the supply of this territory comes from the BA (100 mL/min) and 20% from the contralateral ICaA (26 mL/min).

In a model configuration of a bilateral carotid lesion including an occlusion and a contralateral 50% stenosis with an ACoA diameter ≥1.6 mm, the flow through the still-patent ICaA remains greater than normal (271 mL/min, +9.7% compared with the normal value). Of this amount, 125 mL/min (46.1%) flows to the occluded side through the ACoA. Consequently, the ACeA and MCeA of the nonoccluded side receive only 146 mL/min and an additional 44 mL/min through the ipsilateral PCoA from the BA. The flow in this artery increases from 229 to 331 mL/min (+44.5%), 55 mL/min of which flows to the occluded side through the corresponding PCoA. In this case, the

occluded side still receives more supply from the contralateral ICaA (71%) than from the BA (29%).

In the same configuration of a bilateral carotid lesion but with an ACoA diameter reduced to 0.8 mm, the flow through the patent ICaA is still slightly higher than in the normal case, 237 versus 229 mL/min. Of this amount, 70 mL/min (29.5%) flows to the occluded side through the ACoA. Consequently, the less-occluded side receives only 167 mL/min and an additional 33 mL/min through the ipsilateral PCoA from the BA. The flow in this latter vessel increases from 229 to 344 mL/min (+50%), 80.5 mL/min of which flows to the occluded side through the corresponding PCoA. In this case, the occluded side receives more supply from the BA (53.5%) than from the contralateral ICaA (46.5%). The ACoA diameter threshold at which the supply from the BA equals that from the contralateral ICaA is 0.85 mm.

DISCUSSION

The ACoA has long been suspected of playing a part in the pathogenesis of ischemic lesions due to occlusions and/or stenoses of the ICaAs. As early as 1937, Moniz et al,[29] reporting the first arteriographically documented cases of ICaA occlusion in humans, noted that the clinical consequences of these lesions varied greatly among patients and suggested that the differences could be related to the functional state of the ACoA. Later pathological studies[30 31] reported a trend to a higher occurrence of stringlike ACoAs in patients who died of a cerebral infarction than in patients who were autopsied for other reasons. Recently, Powers[17] gathered some indirect evidence on the effects of the size of ACoA on cerebral hemodynamics.

The well-known variations in form and size of the ACoA[32 33 34] also suggest that this artery could be involved in the mechanisms of the cerebral ischemic lesions induced by ICaA stenoses and occlusions. The diameter of this artery (Table 4; References 35 to 39) was found to vary within the range of 0.1 to 4.9, with a mean value ranging from 1.5 mm[35] to 1.92±0.86 mm.[38] Tulleken[40] considered the “normal” range of the ACoA diameter to be 2.0 to 2.5 mm, but he found this figure in only 20% of the cases he studied. These data have never been discussed in terms of functional significance of this large variability. A common but arbitrary figure was used to classify vessels with an external diameter ≤1 mm as “small” ACoAs. According to this criterion, the frequency of stringlike ACoAs was estimated at 2.9% by Alpers et al[41] in a series of 350 selected normal brains but at 6%,[33] 29%,[34] and 37%[39] in series of unselected autopsy cases.

Our model study shows that these morphometric studies are not suited to a hemodynamic approach to cerebral circulation. There is no threshold diameter of 1 mm that allows separation of “normal” ACoAs from small ones. There are two limits: the upper one corresponds to a diameter of 1.6 mm, above which the ACoA is a fully patent vessel, and the lower one is located at 0.4 mm, below which the ACoA behaves as an occluded vessel. Within this range, 0.4 to 1.6 mm, small changes in ACoA diameter induce significant effects on the intracranial cerebral hemodynamics. We assessed the practical significance of this finding by a further analysis of experimental data previously reported by one of us[38] that are in agreement with most of those mentioned above. This analysis showed that the ACoA diameter was ≥1.6 mm in 18%, ≤0.4 mm in 2%, and between 0.5 and 1.5 mm in 80% of the cases. Even though there is a small difference between the internal diameter, used in our

simulation study, and the external one, usually measured in the morphometric studies,[34 37 38] we can conclude that the ACoA caliber is a factor that deserves to be considered in most cases of severe stenoses or occlusions of the ICaA.

However, in individuals, these limit values could be slightly modified by variations in length, form, and branching of the ACoA, which have not been taken into account in our simulation. The variations in length (Table 4) are known to range from 0 to 10.0 mm, with mean values of 2.5±1.8 mm[37] or 3.3±2.0 mm.[38] Thus, the ACoA appears to be an artery with a length that is small compared with its diameter. Since the resistance in a tube varies linearly with its length and with the reciprocal of the fourth power of its diameter, the effects of these variations in length on the ACoA resistance are negligible compared with those due to variations in diameter. Variations in form of the ACoA are described as being frequent. A single trunk was found in only 60%[35] and 56%[38] of the subjects, while a double trunk was observed in 18%,[33] 33%,[34] 30%,[35] 33.3%,[36] and 33.3%[39] of the subjects. From a mechanical viewpoint, a double trunk has the same effect as a single ACoA with a diameter D ≈1.19 times the diameter d of each segment of the double ACoA. Gomez et al[39] reported mean diameter values of 1.8±0.1 mm in the case of a single trunk and of 1.1±0.1 mm in the case of a double trunk. Thus, in patients with a double trunk, the mean ACoA resistance could be slightly higher than that of patients with a single trunk. Thanks to the operating microscope,[35 36 39 40] it has been recognized that the ACoA invariably has some small (50- to 250-μm) branches. Less frequently, it has a greater branch, which has been described as a midline third anterior cerebral vessel of about the same diameter as the right and left ACeAs, running on the corpus callosum. Such an artery, which was found by Alpers et al[41] in 8% of their patients, is

the only one that could modify the anastomotic role of the ACoA. A specific simulation study is needed to assess the cerebral hemodynamic status associated with this particular configuration.

More importantly, our model does not take into account the variations in size of the PCoAs. The effects of these variations were studied by Hillen and coworkers.[22 26] Using a simplified model of the PCoA,[26] they showed that this artery exhibited a compensatory mechanism that appeared to be independent of its diameter, the flows in the efferent vessels being dominated by the peripheral resistances. Using a complete model of the circle of Willis,[22] they found that doubling the standard size (1 mm) of one of the PCoAs induced very small pressure differences in all segments of the model. They also showed that the flow through one ICaA did not vary as a function of the diameter of both PCoAs within the range of 0.8 to 2.4 mm. However, these simulations were done without any stenosis in the carotid or vertebral arteries, so it would be somewhat hazardous to compare their results with ours. A specific study on this topic remains to be performed. It would concern a relatively small number of patients. Combined anomalies of ACoA and PCoA were reported by Alpers et al[41] to occur in only 13.4% of 360 selected normal brains, and in our own material,[38] the external diameters of all three communicating segments were <1 mm in only 24% of the cases.

Previous simulation studies of the flow in the circle of Willis have shown that the kind of simplifications that are necessary to implement mathematical models did not significantly alter the results provided by these models. Himwich and Clark in dogs[21] and Hillen et al in humans[42] reported data in agreement with experimental[21] and clinical[42] findings. However, none of these studies included the

effects of the anatomic variations of the ACoA on the cerebral hemodynamics in relation to ICaA stenotic or occlusive lesions.

In our study, special attention was paid to the changes in blood pressure within the arterial cerebral network. The transstenotic pressure drop seemed to us to be of importance because it is the first hemodynamic parameter affected by a stenosis and the only one that can be measured in humans. Sillesen et al,[43] in 51 patients undergoing carotid endarterectomy, plotted the “mean pressure gradient” across the stenosis against the degree of stenosis and found a wide range of pressure gradients for each value of stenosis ≥50%. This finding is in agreement with our simulated data, and their Fig 3 looks like our Fig 2 except for two patients in their figure presenting a transstenotic pressure gradient >60 mm Hg, a value that was never reached in our study. However, these two unusually high values of pressure gradient can be due to either a very high MABP or a reduced diameter of the PCoAs, two conditions that were not simulated in our study. Thus, our predicted values of transstenotic pressure drop can be considered realistic enough to deserve further clinical validation studies.

Since we found similar results with the nonlinear unsteady model and the linear one, such studies could be facilitated by the algebraic equation giving the transstenotic pressure drop, ΔP, that we derived from this linear model.

In addition, this equation is of theoretical interest. Since the ACoA conductance varies with the fourth power of the ACoA diameter, the hyperbolic relation between ΔP and the ACoA conductance transforms into an S-shaped curve that lies between a minimum value ΔP_∞ when the ACoA offers minimal resistance to the blood flux and a maximal value ΔP_0 when this resistance tends to infinity. More precisely, for a sufficiently large ACoA diameter, ΔP tends

asymptotically to its minimum value and is as close to it as the fourth power of the reciprocal of the diameter; for a small ACoA caliber, ΔP tends asymptotically to its maximum value and is as close to it as the fourth power of the diameter. It is interesting to note that such a qualitative behavior was observed by Hillen et al for a similar network, although in a different situation[24] and a much simpler H-shaped network,[26] and that we also found double S-shaped curves for the pressure at the level of MCeAs. Thus, one may wonder whether this behavior is a characteristic feature of the pressure distribution, common to a large class of anastomotic networks and similar to the properties of a Wheatstone bridge.[24]

The second pressure parameter we studied was the mean pressure reserve at the entry of the cerebral arteries, which is the true driving force for the cerebral perfusion in each vascular territory. In the normal case, at the lower limit of autoregulation, ie, for an MABP of 60 mm Hg, the pressure reserve at the entry of the MCeA is 22.7 mm Hg. This suggests that a minimum residual pressure of about 22 to 23 mm Hg is required to overcome the vascular resistances of the cerebral arterial network distal to the ACeA and MCeA origin. Below this threshold, the autoregulatory vasodilation of the network could be considered unable to maintain the capillary pressure at the value of 35 mm Hg, which has been shown to be the lowest pressure to maintain the CBF at its normal value.[23]

In the presence of a severe obstructive carotid disease, the MABP required for preserving the autoregulation in a distal vascular territory depends on the ACoA diameter. For instance, in the case of a unilateral occlusion, the MABP value under which the autoregulatory vasodilation would be unable to maintain the capillary pressure at its normal level is ≈66 mm Hg, ie, nearly the same as the “normal” so-called lower limit of autoregulation, when the ACoA

diameter is ≥1.6 mm, while it is ≈111 mm Hg when this diameter is ≤0.4 mm. In both cases, the pressure reserve at the entry of the MCeA is 22.7 mm Hg.

Thus, the mean pressure reserve varies with the severity of the stenotic configuration, the ACoA diameter, and of course the MABP. Fig 6 shows the complexity of these relations. However, two important features should be stressed. First, the mean pressure reserve is nearly a step function of the “cumulated” degree of ICaA stenoses, with a steep decrease from high to low levels around a threshold, ie, a critical stenotic severity. Second, the caliber of the ACoA has a crucial effect on this threshold: the lower the ACoA diameter, the lower the degree of stenosis above which the mean pressure reserve is dramatically reduced. Thus, our study confirms that the diameter of the ACoA is one of the most important factors for the blood pressure regulation in the intracranial cerebral arteries.

CBV and CBF reactivity are linked to the mean pressure reserve in the cerebral arteries. However, an accurate prediction of the relations between these parameters requires a model that includes a more complex simulation of the autoregulatory vasodilatory response of the cerebral network that occurs in response to a reduction in CPP rather than the simplified one we used previously.[23] A realistic simulation of the autoregulation requires a better knowledge than we have of the morphometry of the entire cerebral vascular network, and in particular of the microvasculature.

For the same reasons, we did not simulate the autoregulation in our study of CBF changes. Furthermore, in this first mechanical approach to the hemodynamic effects of the size of the ACoA, it seems better to quantitatively assess the part played by the circle of Willis alone in the compensatory mechanisms that contribute to

maintaining the CBF in the event of severe obstructive lesions of ICaAs.

First, our results suggest that severe stenotic or occlusive ICaA lesions do not induce a significant reduction of the total CBF by themselves and that this reduction could be corrected by a normal autoregulatory vasodilation. This finding is in agreement with clinical data showing that there is no difference in CBF between patients with and without ICaA stenoses and/or occlusion, provided that they have similar cerebral ischemic lesions.[44] The CBF decreases observed in patients with cerebrovascular disease could only be due to either a reduced metabolic demand resulting from ischemic lesions of the brain tissue or hemodynamic factors such as an increase in peripheral resistances or in blood viscosity.

Second, all the efferent and communicating arteries of the circle of Willis are involved in the compensatory mechanisms that cope with the deficit in the more stenotic vessel, but the part played by each vessel depends on the anatomic configuration. When the diameter of both PCoAs is kept at its normal value of 1 mm, the CBF increases that occur in the afferent and communicating arteries are more marked in the ICaA contralateral to the main lesion than in the BA and are more marked in the ACoA than in the PCoAs. The highest flows through the communicating arteries were 199 mL/min, ie, 80% of the normal flow in an ICaA, for the ACoA but only 102 mL/min, ie, 41% of this normal flow, for a PCoA. Thus, the anterior part of the circle of Willis appears to be the main collateral pathway in the event of severe stenotic or occlusive ICaA lesions. However, this holds only if the ACoA diameter is >0.75 mm for unilateral ICaA stenoses and >0.85 mm for severe bilateral lesions. On the whole, the CBF increases that occur in the arteries of the base of the skull are high enough to compensate almost fully for the deficit in the

more stenotic vessel. This means that the circle of Willis, since it behaves as a pressure equalizer, takes an important part in the CBF autoregulation before the vasodilatation of the resistive arteries is involved.

The practical value of our results depends mainly on the possibility of accurately assessing the ACoA diameter in each patient. Magnetic resonance angiography has been applied to the study of blood flow dynamics in the circle of Willis[45] and to the evaluation of patients with intracranial aneurysms, arteriovenous malformations, dural sinus occlusions, and large-vessel atherosclerotic disease.[46] However, to the best of our knowledge, magnetic resonance angiography has never been applied to a morphometric assessment of the ACoA, because its spatial resolution is not high enough to allow for measurement of blood vessel diameters to within 0.1 mm. In particular, double ACoAs, the occurrence of which is 33%, have never been described with this technique.

Two comments of practical interest can be derived from our data. The first concerns the patients with a unilateral ICaA stenosis of ≥70%, who have been found, as a whole, to benefit from carotid endarterectomy.[47 48] These groups obviously included patients with the whole range of ACoA diameters. As shown by our study, patients with a very small ACoA are characterized by a residual pressure in the carotid territory below the lower limit of autoregulation, except if the MABP is significantly increased, whereas patients with a large ACoA have a residual pressure in the carotid territory over the lower limit of autoregulation quite similar to that of normal subjects. Furthermore, patients with a small ACoA have a blood flow through the stenotic ICaA that is relatively less decreased than that of patients with a large ACoA. For instance, patients with a 70%

unilateral ICaA stenosis have an ipsilateral ICaA blood flow of 30 mL/min or of 75 mL/min when their ACoA diameter is ≥1.6 mm or is equal to 0.5 mm, respectively. It can be deduced from these values that the wall shear stress at the stenosis, which is likely to involve an increased risk of embolus release, is doubled when the ACoA diameter is very small compared with when it is large. The patients with a small ACoA are therefore at higher risk of stroke than patients with a clearly patent ACoA, but the ACoA threshold that would allow separation of the two groups depends on the degree of ICaA stenosis. Our simulated data suggest that this threshold could be located at an ACoA diameter of 0.7 mm for a unilateral ICaA stenosis of 70% and of 0.9 mm for a unilateral stenosis of ≥95%. In the series of 100 circles of Willis[38] we had the opportunity to analyze, 19% of the subjects had an ACoA diameter <0.8 mm and 35% <0.9 mm. This pattern deserves to be compared with the results of the multicenter trial of carotid endarterectomy, which showed a cumulative total risk of 21.9% at 3 years[47] and a cumulative risk of any ipsilateral stroke of 26% at 2 years[48] in medically treated patients.

Our second comment concerns patients with an ICaA occlusion associated with a contralateral stenosis. These patients have very high blood flow and wall shear stress through the stenotic ICaA, a situation that is likely to involve an increased risk of embolus release from the stenotic lesion. Furthermore, the threshold over which the residual pressure falls below the lower limit of autoregulation occurs within a very short range of carotid stenosis, 30% to 50%, whatever the MABP and the ACoA diameter are. Consequently, these patients are to be considered at high risk of stroke on the stenotic side, since the degree of stenosis reaches 30%.

SELECTED ABBREVIATIONS AND ACRONYMS

ACeA	=	anterior cerebral artery
ACoA	=	anterior communicating artery
BA	=	basilar artery
CBF	=	cerebral blood flow
CBV	=	cerebral blood volume
CPP	=	cerebral perfusion pressure
ICaA	=	internal carotid artery
MABP	=	mean arterial blood pressure
MCeA	=	middle cerebral artery
PCeA	=	posterior cerebral artery
PCoA	=	posterior communicating artery
tCBF	=	total cerebral blood flow

APPENDIX A

Basic Equations for the Nonlinear Unsteady Model

Blood flow in each vessel of the network is governed by the following set of

\batchmode \documentclass[fleqn,10pt,legalpaper]{article} \usepackage{amssymb} \usepackage{amsfonts} \usepackage{amsmath} \pagestyle{empty} \begin{document} \[\ Continuity:\ \frac{{\partial}A}{{\partial}t}{+}\frac{{\partial}Q}{{\partial}z} {=}0\] \end{document}

\batchmode \documentclass[fleqn,10pt,legalpaper]{article} \usepackage{amssymb} \usepackage{amsfonts} \usepackage{amsmath} \pagestyle{empty} \begin{document} \[\ Momentum:\ \frac{{\partial}Q}{{\partial}t}{+}\frac{{\partial}}{{\partial}z}

({\alpha}\frac{Q^{2}}{A}){=}{-}\frac{A}{{\rho}}\ \frac{{\partial}p}{{\partial}z}{+}\frac{2{\pi}}{{\rho}}\ R{\tau}_{w}\] \end{document}

\batchmode \documentclass[fleqn,10pt,legalpaper]{article} \usepackage{amssymb} \usepackage{amsfonts} \usepackage{amsmath} \pagestyle{empty} \begin{document} \[\ Tube\ law:\ A{=}A(p,z,t)\] \end{document}

These equations relate the variable cross-sectional area (A) of a distensible vessel, the pressure (p), the flow rate (Q), and the wall shear stress (τ_w), which are the fluid mechanical variables of the problem; in these equations, R is the tube radius, and α, the momentum shape factor, is taken to be equal to unity (flat velocity profile).

An approximation of τ_w in an unsteady flow must be provided to close the system, ie, to have an equal number of unknowns and equations. For medium-size arteries, such as the carotid and cerebral arteries, the following second-order asymptotic expression was found to be satisfactory:

\batchmode \documentclass[fleqn,10pt,legalpaper]{article} \usepackage{amssymb} \usepackage{amsfonts} \usepackage{amsmath} \pagestyle{empty} \begin{document} \ [\frac{Q}{{\pi}R^{3}}{+}\frac{1}{16{\mu}}\ \frac{{\rho}}{{\pi}R}\ \frac{{\partial}Q}{{\partial}t}{=}{-}\frac{1}{4{\mu}}{\tau}_{w}\ {-}\frac{1}{192{\mu}}\ {\rho}R^{2}\ \frac{{\partial}{\tau}_{w}}{{\partial}t}\] \end{document}

where μ is the dynamic fluid viscosity.

Linear Model

The linear model can be derived by writing the following condition, which expresses mass conservation at each node of the network—ie, each junction of the circle of Willis:

\batchmode \documentclass[fleqn,10pt,legalpaper]{article} \usepackage{amssymb} \usepackage{amsfonts} \usepackage{amsmath} \pagestyle{empty} \begin{document} \[G_{ij}(P_{i}{-}P_{j}){+}G_{ik}(P_{i}{-}P_{k}){+}G_{il}(P_{i}{-}P_{l}){=}S_{i}\] \end{document}

In this equation, P_i, …, are the nodal pressures, and the G_{ij} terms are the conductances of the segments connected to node i, which depend on the fluid viscosity and the vessel geometry. This leads to a cyclic tridiagonal linear system for the nodal pressures that can be solved numerically by standard techniques, provided that the input pressures at the entry of the carotid and vertebral segments and the efferent resistances (the peripheral resistances) are known. This set of nine linear algebraic equations for the nine unknown nodal pressures can be solved analytically by use of the software package for symbolic calculus MAPLE V.

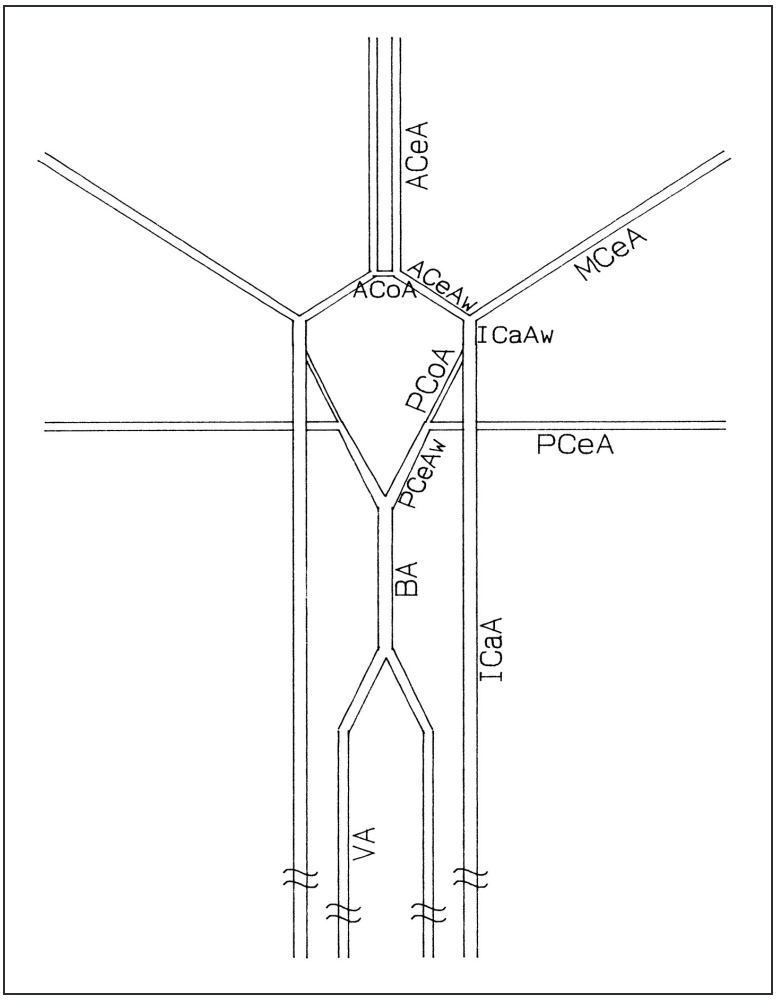

Figure 1. Diagram of our model of the circle of Willis and its afferent and efferent branches. It includes the ICaAs, the vertebral arteries (VAs), the BA, the ACeAs, the ACoA, the MCeAs, the PCeAs, and the PCoAs. The parts of the arteries included in the circle of Willis are marked “w.”

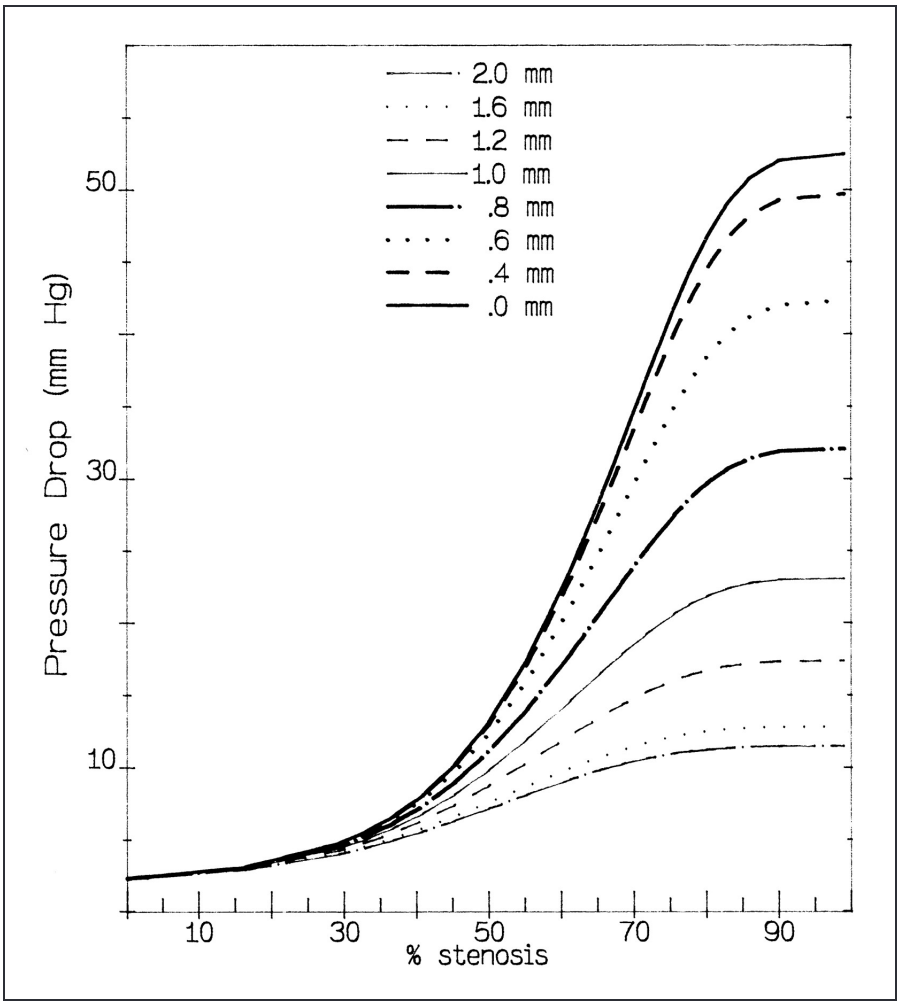

Figure 2. Graph showing mean pressure drop (mm Hg) through an ICaA stenosis vs % ICaA stenosis for eight ACoA diameter values in the range of 0.0 to 2.0 mm.

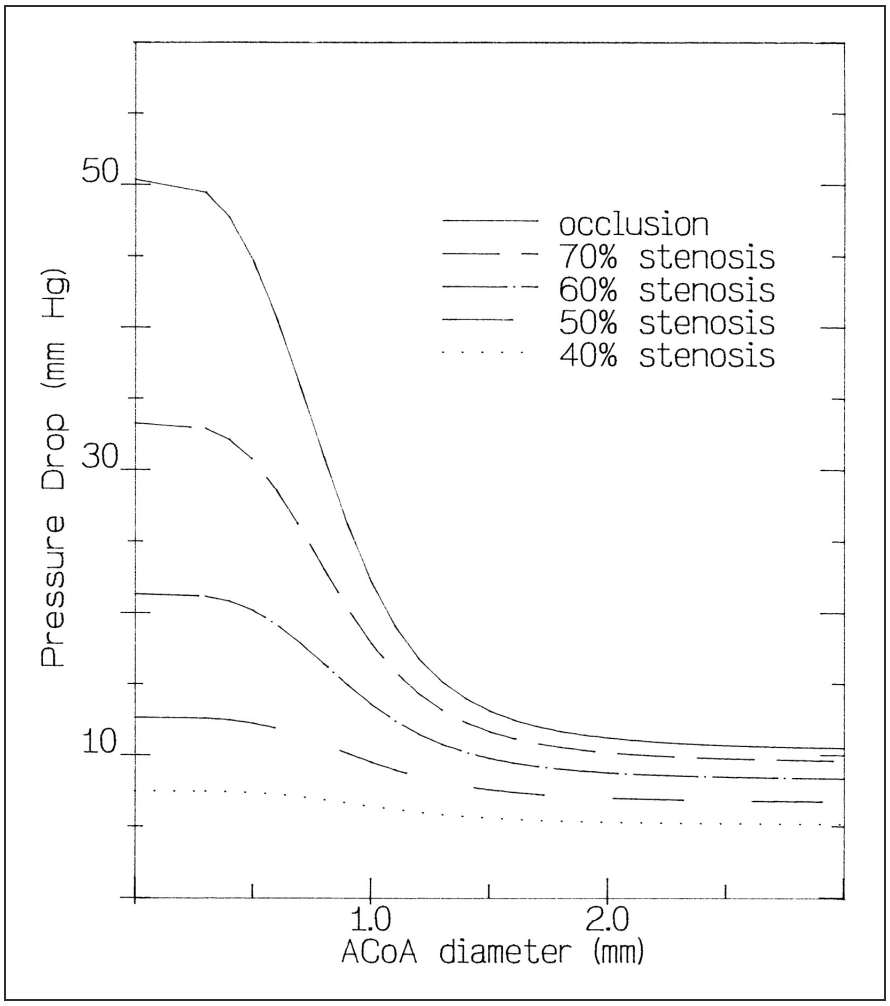

Figure 3. Graph showing mean pressure drop (mm Hg) through an ICaA stenosis vs ACoA diameter (mm) for five degrees of ICaA stenosis in the range of 40% to occlusion.

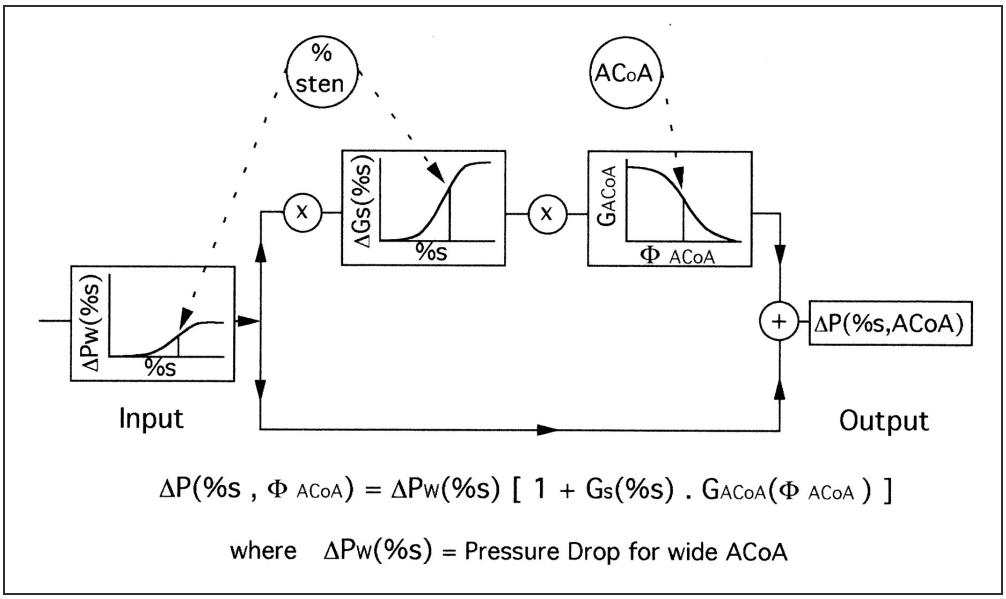

Figure 4. Diagram illustrating the coupling effect of degree of ICaA stenosis (%s, % sten) and of ACoA diameter (Φ ACoA) on the mean pressure drop through an ICaA stenosis. See text for other symbols.

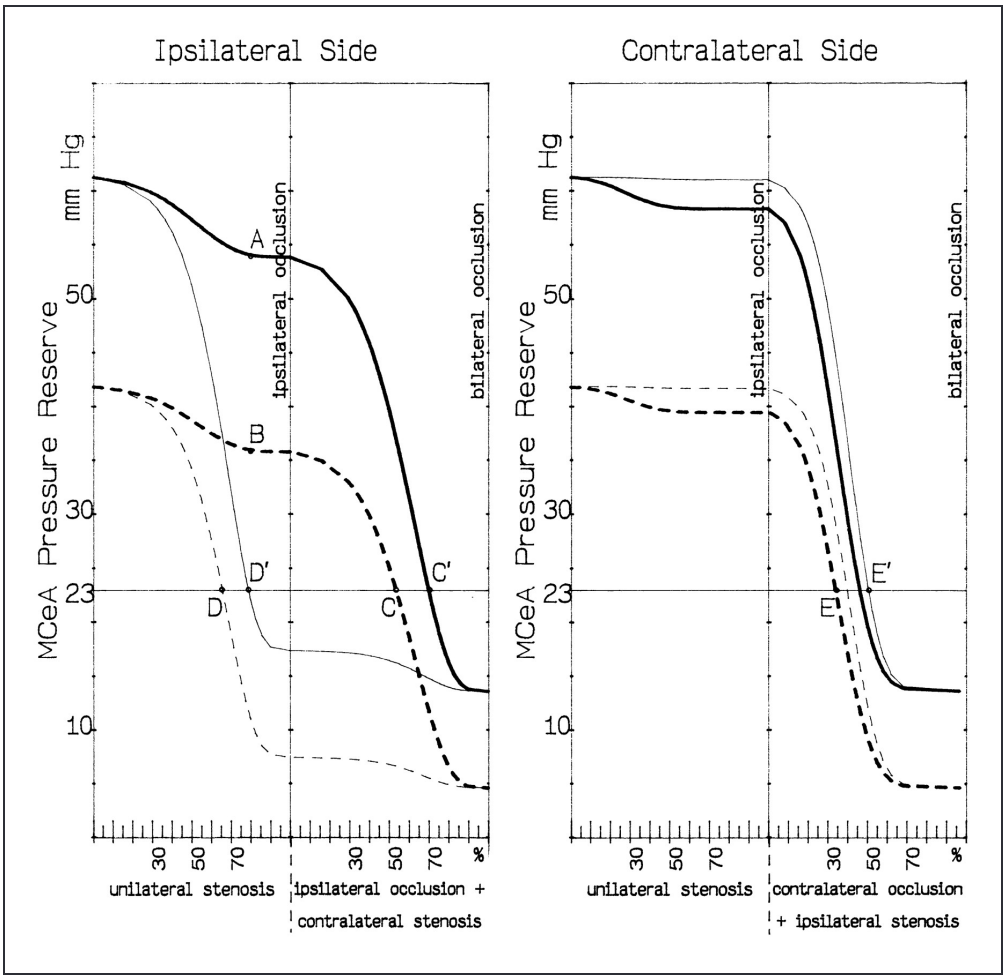

Figure 5. Graphs showing mean pressure reserve (mm Hg) at the entry of the MCeAs ipsilateral and contralateral to the ICaA with the most lesions vs the status of both ICaAs for two values of ACoA diameter (thick line indicates 1.6 mm; thin line, 0.4 mm) and two values of MABP (continuous line, 100 mm Hg; dotted line, 80 mm Hg). For comments on points A, B, C, C′, D, D′, E, E′, see text.

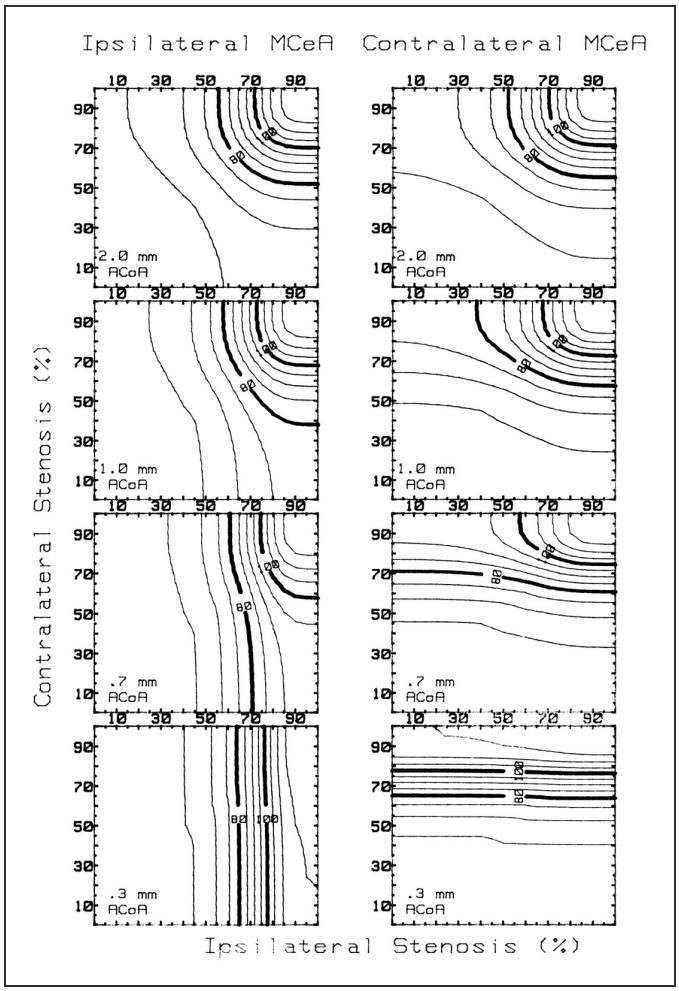

Figure 6. Graphs showing MABP (mm Hg) under which autoregulation is lost in MCeA territories vs the stenotic configuration (%) of both ICaAs for four values of ACoA diameter (A=2.0 mm; B=1.0 mm; C=0.7 mm; and D=0.3 mm).

Table 1. Lengths and Diameters of the Arteries Included in Our Model (Table view)

	Length, mm	Diameter, mm
ICaAs	250	4.00
ICaAs W	20	4.00
Vertebral arteries	200	2.00
BA	30	4.24
ACeAs W	20	2.50
ACeAs	50	2.50
ACoA	5	0.0-3.0
MCeAs	70	3.50
PCeAs W	20	3.00

	Length, mm	Diameter, mm
PCeAs	70	3.00
PCoAs	20	1.00

W indicates parts included in circle of Willis.

Table 2. Blood Flow in the Afferent and Communicating Arteries of the Circle of Willis and in the Network as a Whole (tCBF) Versus Percent of a Unilateral ICaA Lesion (Table view)

	Degree (%) of ICaA Stenosis	iICaA	cICaA	ACoA	BA	iPCoA	cPCoA	tCBF
A. Normal network	0	247	247	0	229	−5	−5	723
B. ACoA=1.6 mm	30	202	280	36	234	0	−3	717
	50	120	340	101	244	8	−1	706
	70	30	407	174	255	18	1	693
	80	7	424	193	258	20	2	690
	100	0	429	199	259	21	2	689
C. ACoA=0.8 mm	30	224	256	9	235	2	−4	716
	50	165	280	35	251	19	−4	698
	70	59	320	77	281	51	−4	661
	80	16	334	91	294	64	−5	645
	100	0	339	97	298	70	−5	638
D. ACoA=0.5 mm	30	231	249	1	235	3	−5	716
	50	184	255	7	254	24	−6	694
	70	75	268	19	296	71	−8	640
	80	23	274	24	315	92	−9	613
	100	0	277	26	323	100	−9	600

i indicates ipsilateral; c, contralateral. Values are mL/min.

Table 3. Blood Flow in the Afferent and Communicating Arteries of the Circle of Willis and in the Network as a Whole (tCBF) Versus Percent of Bilateral ICaA Lesions Including a Variable Lesion and a Fixed Contralateral Stenosis of 50% (Table view)

	Degree (%) of iICaA Stenosis	iICaA	cICaA	ACoA	BA	iPCoA	cPCoA	tCBF

	Degree (%) of iICaA Stenosis	iICaA	cICaA	ACoA	BA	iPCoA	cPCoA	tCBF
A. ACoA=1.6 mm	30	292	143	0	256	7	13	692
	50	190	190	0	282	24	24	662
	70	56	248	88	316	46	38	620
	80	14	265	116	327	53	43	607
	100	0	271	125	331	55	44	602
B. ACoA=0.8 mm	30	256	172	0	260	3	20	688
	50	190	190	0	282	24	24	662
	70	68	221	46	322	60	30	612
	80	19	233	63	338	75	32	591
	100	0	237	70	344	81	33	582
C. ACoA=0.5 mm	30	239	185	0	261	1	24	686
	50	190	190	0	282	24	24	662
	70	77	200	12	327	72	24	605
	80	23	204	18	347	93	23	575
	100	0	206	20	355	102	23	562

i indicates ipsilateral; c, contralateral. Values are mL/min.

Table 4. Morphometric Data on the ACoA (Table view)

Reference	No. of Subjects	Diameter, mm		Length, mm	
		Range	Mean±SD	Range	Mean±SD
Fisher,[34] 1965	414	0.25-3.0		0.0-7.0	
Perlmutter and Rhoton,[35] 1976	50	0.20-3.4	1.50	0.3-7.0	2.6
Crowell and Morawetz,[36] 1977	10	0.80-2.3		5.0±10.0	
Kamath,[37] 1981	100	0.40-4.9	1.90 ±0.90	0.5-10.4	2.5±1.8
Hillen,[38] 1986	100	0.10-4.7	1.92±0.86		3.3±2.0
Gomes et al,[39] 1986	30		1.80±0.10[1]		3.9 ±0.4[1]

[1] In case of a single trunk.

ARTICLE INFORMATION

Received April 17, 1995; accepted June 23, 1995.

Correspondence

Correspondence to J.-P. Marc-Vergnes, INSERM U.230, Service de Neurologie, CHU Purpan, 31059 Toulouse Cédex, France.

Affiliations

From INSERM U.230, Service de Neurologie, CHU Purpan (F.C., V.V., P.B., M.Z., J.-P.M.-V.), Toulouse, France; the Laboratoire de Modélisation en Mécanique des Fluides, Université Paul-Sabatier (V.V., M.Z.), Toulouse, France; and Department of Functional Anatomy, University of Utrecht (B.H.), Netherlands. .

Acknowledgments

We would like to thank Dr P. Celsis and Pr F. Chollet for their valuable comments, Dr I. Berry for her advice on magnetic resonance angiography, and I. Delcroix for preparing the manuscript.

REFERENCES

1. Gibbs JM, Wise RJS, Leenders KL, Jones T. Evaluation of cerebral perfusion reserve in patients with carotid artery occlusion. *Lancet.* 1984;*1*:310-314. Crossref. PubMed.
2. Powers WJ, Press GA, Grubb RL Jr, Gado M, Raichle ME. The effect of hemodynamically significant carotid disease on the hemodynamic status of the cerebral circulation. *Ann Intern Med.* 1987;*106*:27-35. Crossref. PubMed.
3. Derlon JM, Bouvard G, Hubert P, Lechevalier B, Dupuy B, Viader F, Maiza D, Courthéoux P, Fernandez Y, Houtteville JP. Etude hémodynamique des lésions obstructives de l'artère carotide interne: intérêt de la mesure couplée du débit et du volume sanguins cérébraux régionaux. *Rev Neurol (Paris).* 1987;*143*:32-39. PubMed.
4. Leblanc R, Yamamoto YL, Tyler JL, Hakim A. Hemodynamic and metabolic effects of extracranial carotid disease. *Can J Neurol Sci.* 1989;*16*:51-57. Crossref. PubMed.
5. Sette G, Baron JC, Mazoyer B, Levasseur M, Pappata S, Crouzel C. Local brain haemodynamics and oxygen metabolism in cerebrovascular disease: positron emission tomography. *Brain.* 1989;*112*:931-951. Crossref. PubMed.

6. Toyama H, Takeshita G, Takeuchi A, Anno H, Ejiri K, Maeda H, Katada K, Koga S, Ishiyama N, Kanno T, Yamaoka N. Cerebral hemodynamics in patients with chronic obstructive carotid disease by rCBF, rCBV, and rCBV/CBF ratio using SPECT. *J Nucl Med.* 1990;*31*:55-60. PubMed.
7. Sabatini U, Celsis P, Viallard G, Rascol A, Marc-Vergnes JP. Quantitative assessment of cerebral blood flow by single-photon emission computed tomography. *Stroke.* 1991;*22*:324-330. Crossref. PubMed.
8. Bloor BM, Asli RP, Nugent GR, Majzoub HS. Relationship of cerebrovascular reactivity to degree of extracranial vascular occlusion. *Circulation*. 1966;33/34(suppl II):II-28-II-34.
9. Norrving B, Nilsson MD, Risberg J. rCBF in patients with carotid occlusion: resting and hypercapnic flow related to collateral pattern. *Stroke.* 1982;*13*:155-162. Crossref. PubMed.
10. Brown MM, Wade JPH, Bishop CCR, Ross Russell RW. Reactivity of the cerebral circulation in patients with carotid occlusion. *J Neurol Neurosurg Psychiatry.* 1986;*79*:899-904.
11. Levine RL, Dobkin JA, Rozental JM, Satter MR, Nickles RJ. Blood flow reactivity to hypercapnia in strictly unilateral carotid disease: preliminary results. *J Neurol Neurosurg Psychiatry.* 1991;*54*:204-209. Crossref. PubMed.
12. Vorstrup S. Tomographic cerebral blood flow measurements in patients with ischemic cerebrovascular disease and evaluation of the vasodilatory capacity by the acetazolamide test. *Acta Neurol Scand.* 1988;*77*:1-47. Crossref. PubMed.
13. Chollet F, Celsis P, Clanet M, Guiraud-Chaumeil B, Rascol A, Marc-Vergnes JP. SPECT study of cerebral blood flow reactivity after acetazolamide in patients with transient ischemic attacks. *Stroke.* 1989;*20*:458-464. Crossref. PubMed.
14. Knop J, Thie A, Fuchs C, Siepmann G, Zeumer H.^{99m}Tc-HMPAO-SPECT with acetazolamide challenge to detect hemodynamic compromise in occlusive cerebrovascular disease. *Stroke.* 1992;*23*:1733-1742. Crossref. PubMed.
15. Herold S, Brown MM, Frackowiak RSJ, Mansfield AO, Thomas DJ, Marshall J. Assessment of cerebral hemodynamic reserve: correlation between PET parameters and CO_2 reactivity measured by intravenous ^{133}xenon injection technique. *J Neurol Neurosurg Psychiatry.* 1988;*51*:1040-1050.
16. Grubb RL Jr, Phelps ME, Raichle ME, Ter-Pogossian MM. The effects of arterial blood pressure on the regional blood volume by x-ray fluorescence. *Stroke.* 1973;*4*:390-399. Crossref. PubMed.
17. Powers WJ. Cerebral hemodynamics in ischemic cerebrovascular disease. *Ann Neurol.* 1991;*29*:231-240. Crossref. PubMed.

18. Schroeder T. Hemodynamic significance of internal carotid artery disease. *Acta Neurol Scand.* 1988;*77*:353-372. Crossref. PubMed.
19. Himwich WA, Knapp FM, Wenglarz RA, Martin JD, Clark ME. The circle of Willis as simulated by an engineering model. *Arch Neurol.* 1965;*13*:164-172. Crossref. PubMed.
20. Clark ME, Himwich WA, Martin JD. A comparative examination of cerebral circulation models. *J Neurosurg.* 1968;*29*:484-494. Crossref.
21. Himwich WA, Clark ME. Cerebral blood flow comparisons between model and prototype. *J Appl Physiol.* 1971;*31*:873-879. Crossref. PubMed.
22. Hillen B, Hoogstraten HW, Post L. A mathematical model of the flow in the circle of Willis. *J Biomech.* 1986;*19*:187-194. Crossref. PubMed.
23. Zagzoule M, Marc-Vergnes JP. A global mathematical model of the cerebral circulation in man. *J Biomech*. 1986;19;1015-1021.
24. Hillen B, Drinkenburg AH, Hoogstraten HW, Post L. Analysis of flow and vascular resistance in a model of the circle of Willis. *J Biomech.* 1988;*21*:807-814. Crossref. PubMed.
25. Zagzoule M, Khalid-Naciri J, Mauss J. Unsteady wall shear stress in a distensible tube. *J Biomech.* 1991;*24*:435-439. Crossref. PubMed.
26. Hillen B, Gaasbeek T, Hoogstraten HW. A mathematical model of the flow in the posterior communicating artery. *J Biomech.* 1982;*15*:441-448. Crossref. PubMed.
27. Young DF, Tsai FY. Flow characteristics in models of arterial stenoses, II: unsteady flow. *J Biomech.* 1973;*6*:547-559. Crossref. PubMed.
28. Young DF, Cholvin NR, Roth AC. Pressure drop across artificially induced stenoses in the femoral arteries of dogs. *Circ Res.* 1977;*36*:735-743.
29. Moniz E, Lima A, de Lacerda R. Hémiplégies par thrombose de la carotide interne. *Presse Med.* 1937;*52*:977-980.
30. Fettermen GH, Moran TJ. Anomalies of the circle of Willis in relation to cerebral softening. *Arch Pathol.* 1941;*32*:251-257.
31. Battacharji SK, Hutchinson EC, McCall AJ. The circle of Willis: the incidence of developmental abnormalities in normal and infarcted brains. *Brain.* 1967;*90*:747-758. Crossref. PubMed.
32. Fawcett E, Blachford JV. The circle of Willis: an examination of 700 specimens. *J Anat Physiol.* 1906;*20*:63-70.
33. De Almeida FP. Distribuição na superficia do cérebro das artérias cérebral anterior e comunicante anterior. *Arq Anat Antropol.* 1934;*16*:323-353.
34. Fisher CM. The circle of Willis: anatomical variations. *Vasc Dis.* 1965;*2*:99-105.
35. Perlmutter D, Rhoton AL Jr. Microsurgical anatomy of the anterior cerebral-anterior

communicating-recurrent artery complex. *J Neurosurg.* 1976;*45*:259-272. Crossref. PubMed.

36. Crowell RM, Morawetz RB. The anterior communicating artery has significant branches. *Stroke.* 1977;*8*:272-273. Crossref. PubMed.
37. Kamath S. Observations on the length and diameter of vessels forming the circle of Willis. *J Anat.* 1981;*133*:419-423. PubMed.
38. Hillen B. The variability of the circle of Willis: univariate and bivariate analysis. *Acta Morphol Neerl Scand.* 1986;*24*:87-101. PubMed.
39. Gomez FB, Dujovny M, Umansky F, Berman SK, Diaz FG, Ausman JI, Lirchandani HG, Ray WJ. Microanatomy of the anterior cerebral artery. *Surg Neurol.* 1986;*26*:129-141. Crossref. PubMed.
40. Tulleken CAF. A study of the anatomy of the anterior communicating artery with the aid of the operating microscope. *Clin Neurol Neurosurg.* 1977;*80*:169-173.
41. Alpers BJ, Berry RG, Paddison RM. Anatomical studies of the circle of Willis in the normal brain. *Arch Neurol Psychiatry.* 1959;*81*:409-418. Crossref.
42. Hillen B, Hoogstraten HW, Van Overbeeke JJ, Van der Zwan A. Functional anatomy on the circulus arteriosus cerebri (Willisid). *Bull Assoc Anat (Nancy).* 1991;*75*:123-126.
43. Sillesen H, Schroeder T, Steenberg HJ, Buchardt Hansen HJ. Doppler examination of the periorbital arteries adds valuable hemodynamic information in carotid artery disease. *Ultrasound Med Biol.* 1987;*13*:177-181. Crossref. PubMed.
44. Géraud J, Bès A, Rascol A, Delpla M, Marc-Vergnes JP, Lazorthes Y. Les mesures du débit sanguin cérébral dans les sténoses et les thrombose de la carotide interne: etude critique de leurs possibilités. *Rev Neurol.* 1966;*115*:695-702. PubMed.
45. Edelman RR, Mattle HP, O'Reilly GV, Wentz KU, Liu C, Zhao B. Magnetic resonance imaging flow dynamics in the circle of Willis. *Stroke.* 1990;*21*:56-65. Crossref. PubMed.
46. Ruggieri PM, Masaryk TJ, Ross JS. Magnetic resonance angiography: cerebrovascular applications. *Stroke.* 1992;*23*:774-780. Crossref. PubMed.
47. European Carotid Surgery Trialists' Collaborative Group: MRC European Surgery Trial: interim results for symptomatic patients with severe (70-99%) or with mild (0-29%) carotid stenosis. *Lancet.* 1991;*337*:1235-1243. Crossref. PubMed.
48. NASCET Collaborators. Beneficial effect of carotid endarterectomy in symptomatic patients with high grade stenosis. *N Engl J Med.* 1991;*325*:445-453. Crossref. PubMed.

Sections

LIST OF ILLUSTRATIONS

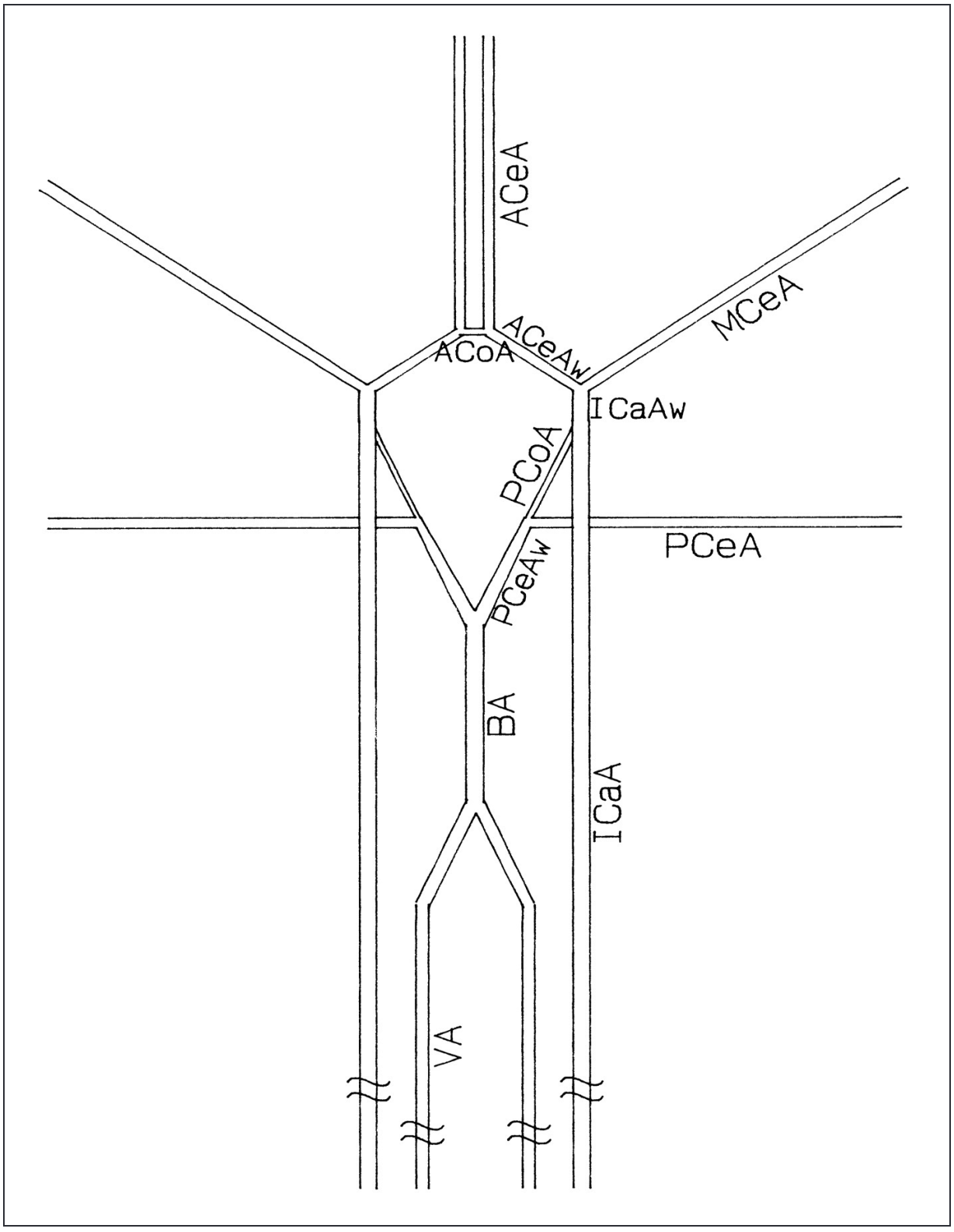
ACeA
MCeA
ACoA
ACeAw
ICaAw
PCoA
PCeA
PCeAw
BA
ICaA
VA

Figure 1. Diagram of our model of the circle of Willis and its afferent and efferent branches. It includes the ICaAs, the vertebral arteries (VAs), the BA, the ACeAs, the ACoA, the MCeAs, the PCeAs, and the PCoAs. The parts of the arteries included in the circle of Willis are marked “w.”

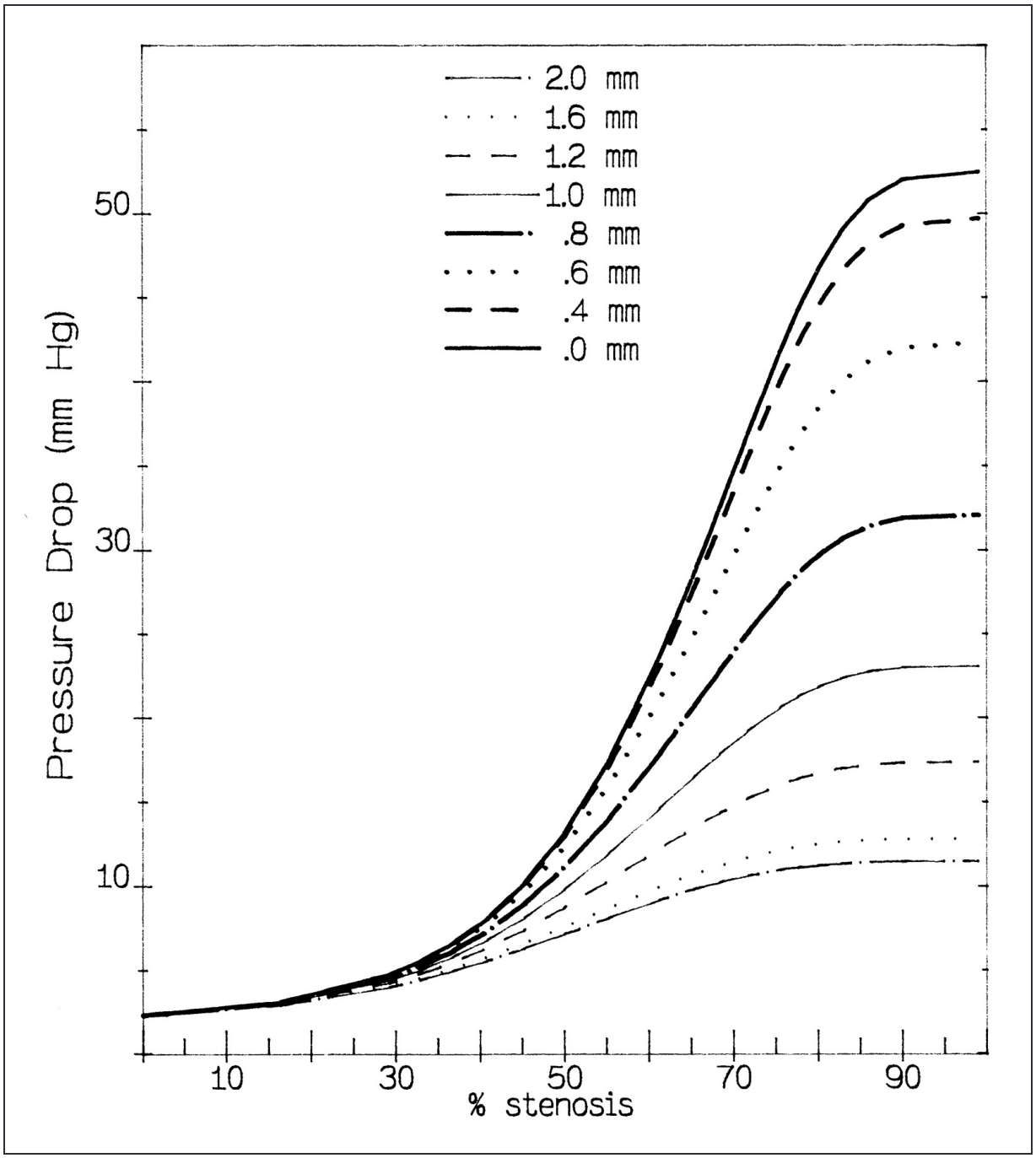

Figure 2. Graph showing mean pressure drop (mm Hg) through an ICaA stenosis vs % ICaA stenosis for eight ACoA diameter values in the range of 0.0 to 2.0 mm.

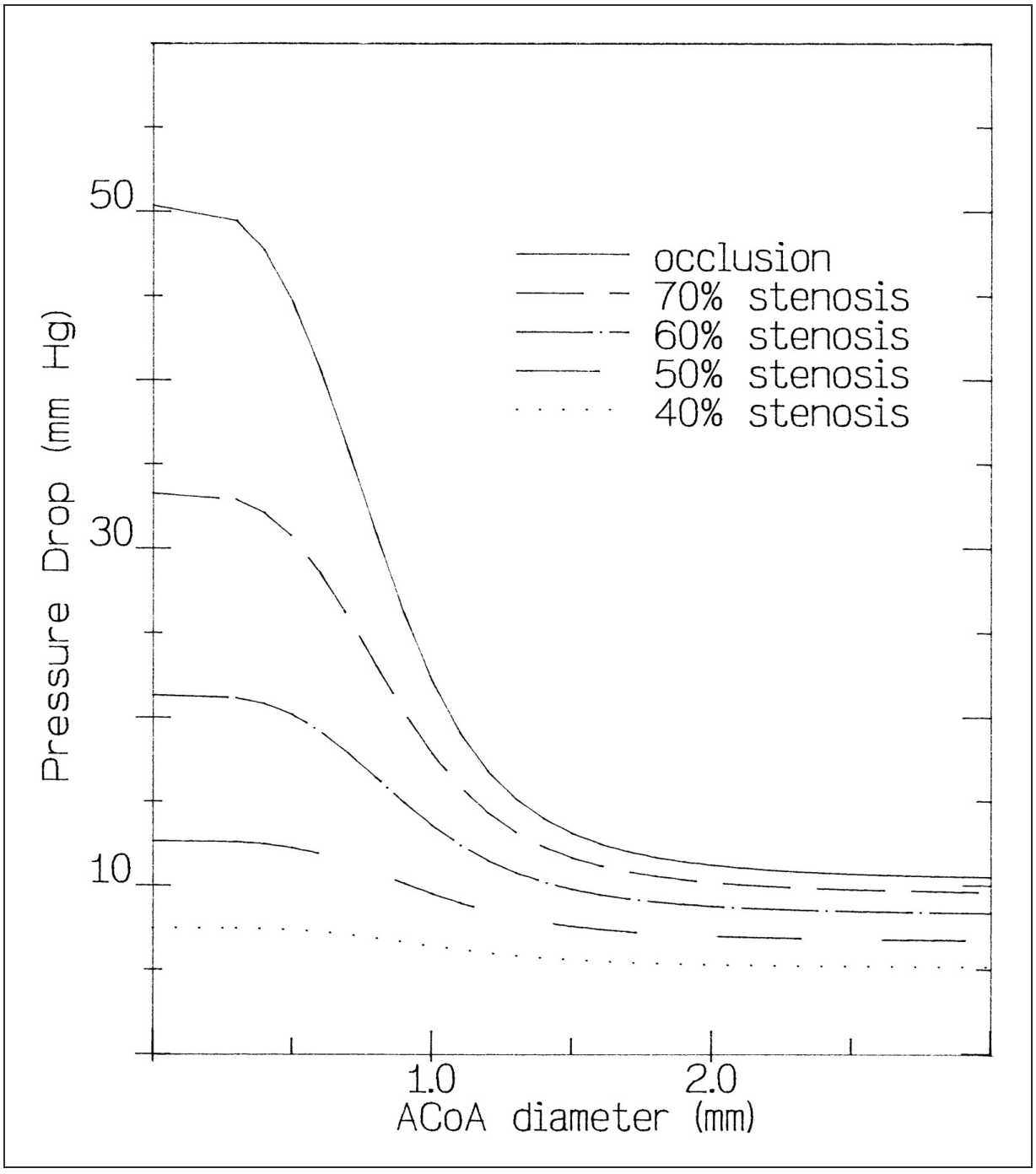

Figure 3. Graph showing mean pressure drop (mm Hg) through an ICaA stenosis vs ACoA diameter (mm) for five degrees of ICaA stenosis in the range of 40% to occlusion.

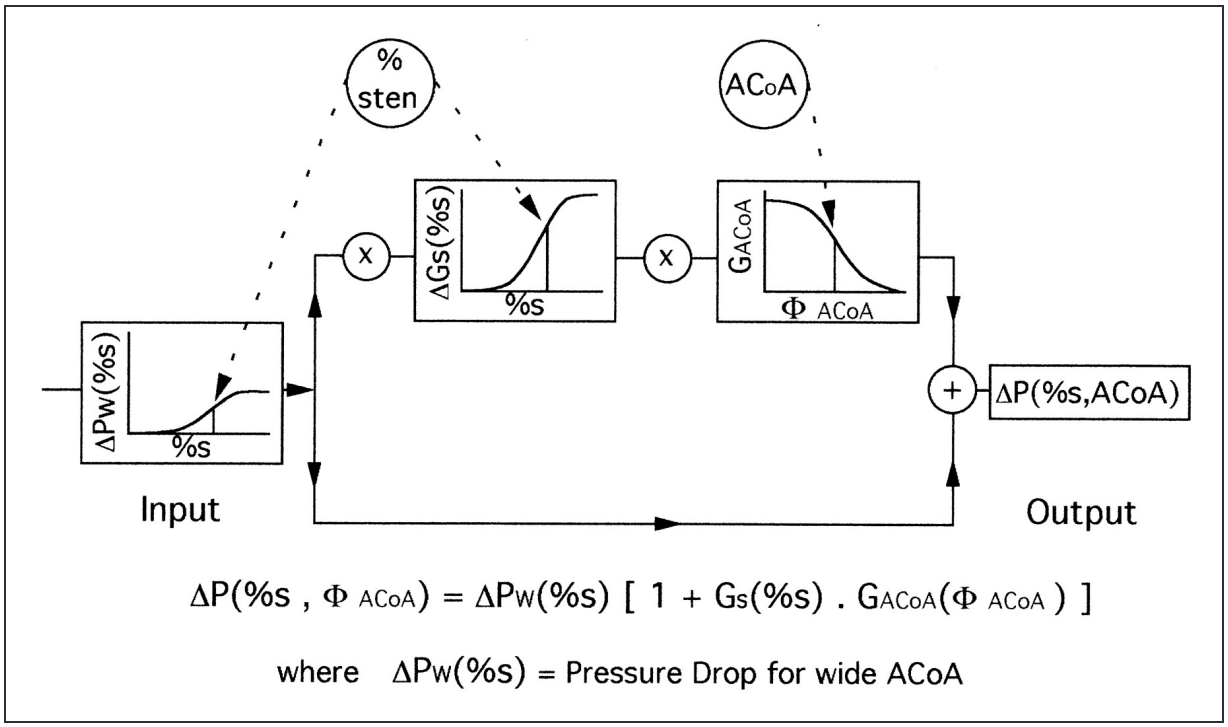

Figure 4. Diagram illustrating the coupling effect of degree of ICaA stenosis (%s, % sten) and of ACoA diameter (Φ ACoA) on the mean pressure drop through an ICaA stenosis. See text for other symbols.

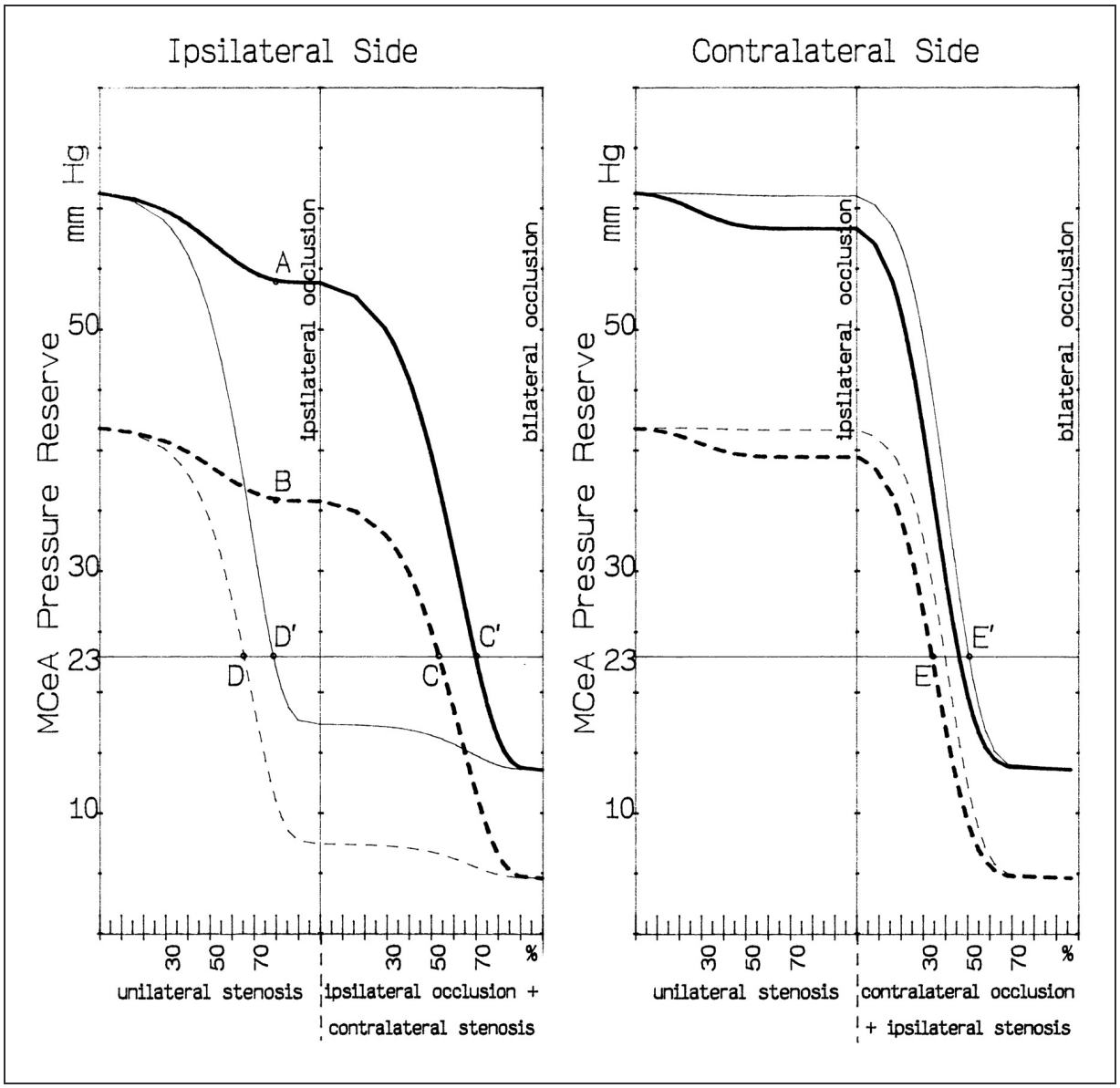

Figure 5. Graphs showing mean pressure reserve (mm Hg) at the entry of the MCeAs ipsilateral and contralateral to the ICaA with the most lesions vs the status of both ICaAs for two values of ACoA diameter (thick line indicates 1.6 mm; thin line, 0.4 mm) and two values of MABP (continuous line, 100 mm Hg; dotted line, 80 mm Hg). For comments on points A, B, C, C′, D, D′, E, E′, see text.

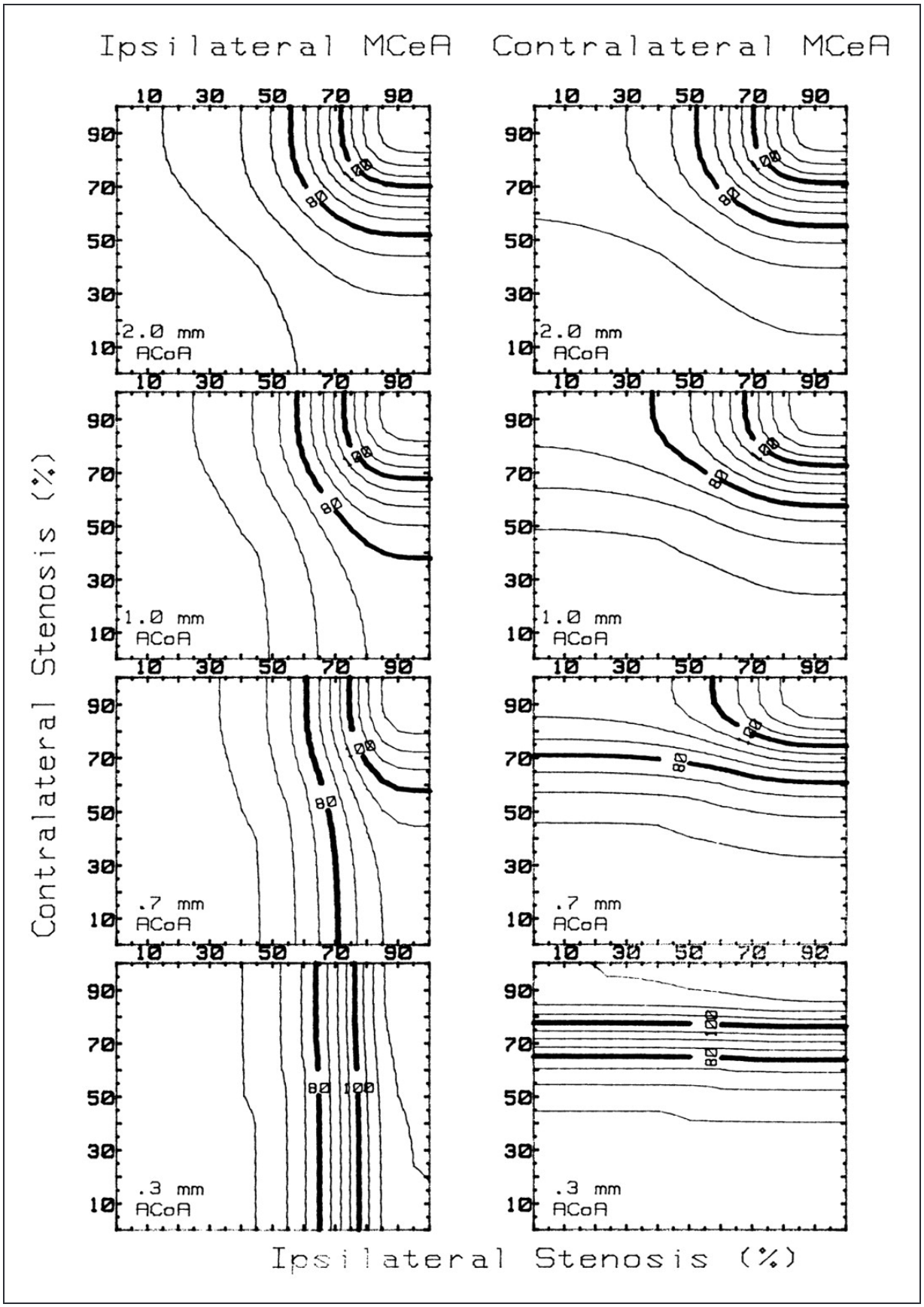
Ipsilateral MCeA
Contralateral MCeA
Contralateral Stenosis (%)
Ipsilateral Stenosis (%)
10 30 50 70 90
90
70
50
30
10
80
100
2.0 mm ACoA
1.0 mm ACoA
.7 mm ACoA
.3 mm ACoA

Figure 6. Graphs showing MABP (mm Hg) under which autoregulation is lost in MCeA territories vs the stenotic configuration (%) of both ICaAs for four values of ACoA diameter (A=2.0 mm; B=1.0 mm; C=0.7 mm; and D=0.3 mm).

ACeA	=	anterior cerebral artery
ACoA	=	anterior communicating artery
BA	=	basilar artery
CBF	=	cerebral blood flow
CBV	=	cerebral blood volume
CPP	=	cerebral perfusion pressure
ICaA	=	internal carotid artery
MABP	=	mean arterial blood pressure
MCeA	=	middle cerebral artery
PCeA	=	posterior cerebral artery
PCoA	=	posterior communicating artery
tCBF	=	total cerebral blood flow

Table 1. Lengths and Diameters of the Arteries Included in Our Model

	Length, mm	Diameter, mm
ICaAs	250	4.00
ICaAs W	20	4.00
Vertebral arteries	200	2.00
BA	30	4.24
ACeAs W	20	2.50
ACeAs	50	2.50
ACoA	5	0.0-3.0
MCeAs	70	3.50
PCeAs W	20	3.00
PCeAs	70	3.00
PCoAs	20	1.00

W indicates parts included in circle of Willis.

Table 2. Blood Flow in the Afferent and Communicating Arteries of the Circle of Willis and in the Network as a Whole (tCBF) Versus Percent of a Unilateral ICaA Lesion

	Degree (%) of ICaA Stenosis	iICaA	cICaA	ACoA	BA	iPCoA	cPCoA	tCBF
A. Normal network	0	247	247	0	229	−5	−5	723
B. ACoA=1.6 mm	30	202	280	36	234	0	−3	717
	50	120	340	101	244	8	−1	706
	70	30	407	174	255	18	1	693
	80	7	424	193	258	20	2	690
	100	0	429	199	259	21	2	689
C. ACoA=0.8 mm	30	224	256	9	235	2	−4	716
	50	165	280	35	251	19	−4	698
	70	59	320	77	281	51	−4	661
	80	16	334	91	294	64	−5	645
	100	0	339	97	298	70	−5	638
D. ACoA=0.5 mm	30	231	249	1	235	3	−5	716
	50	184	255	7	254	24	−6	694
	70	75	268	19	296	71	−8	640
	80	23	274	24	315	92	−9	613
	100	0	277	26	323	100	−9	600

i indicates ipsilateral; c, contralateral. Values are mL/min.

Table 3. Blood Flow in the Afferent and Communicating Arteries of the Circle of Willis and in the Network as a Whole (tCBF) Versus Percent of Bilateral ICaA Lesions Including a Variable Lesion and a Fixed Contralateral Stenosis of 50%

	Degree (%) of iICaA Stenosis	iICaA	cICaA	ACoA	BA	iPCoA	cPCoA	tCBF
A. ACoA=1.6 mm	30	292	143	0	256	7	13	692
	50	190	190	0	282	24	24	662
	70	56	248	88	316	46	38	620
	80	14	265	116	327	53	43	607
	100	0	271	125	331	55	44	602
B. ACoA=0.8 mm	30	256	172	0	260	3	20	688
	50	190	190	0	282	24	24	662
	70	68	221	46	322	60	30	612
	80	19	233	63	338	75	32	591
	100	0	237	70	344	81	33	582
C. ACoA=0.5 mm	30	239	185	0	261	1	24	686
	50	190	190	0	282	24	24	662
	70	77	200	12	327	72	24	605
	80	23	204	18	347	93	23	575
	100	0	206	20	355	102	23	562

i indicates ipsilateral; c, contralateral. Values are mL/min.

Table 4. Morphometric Data on the ACoA

Reference	No. of Subjects	Diameter, mm		Length, mm	
		Range	Mean±SD	Range	Mean±SD
Fisher,[34] 1965	414	0.25-3.0		0.0-7.0	
Perlmutter and Rhoton,[35] 1976	50	0.20-3.4	1.50	0.3-7.0	2.6
Crowell and Morawetz,[36] 1977	10	0.80-2.3		5.0±10.0	
Kamath,[37] 1981	100	0.40-4.9	1.90 ±0.90	0.5-10.4	2.5±1.8
Hillen,[38] 1986	100	0.10-4.7	1.92±0.86		3.3±2.0
Gomes et al,[39] 1986	30		1.80±0.10[1]		3.9 ±0.4[1]

[1] In case of a single trunk.